Observation of Loop Connectivity Change in a Solar Flare Triggered by Loop-Loop Interaction

Linhui Sui[1,2], Gordon D. Holman[2], and Brian R. Dennis[2]

ABSTRACT

Magnetic reconnection between two adjacent magnetic loops or arcades has been a longstanding model for solar flares. However, the observations supporting this quadrupolar flare model are mainly post-reconnection observations. We present a set of flare observations in EUV, X-rays and Hα which shows that a pre-flare loop changed its connectivity soon after the start of an M1 flare on June 2, 2002. A large arcade of loops seen in EUV expanded slowly at $\sim$6 km s^{-1} about 3 min before the start of the flare. Another smaller EUV loop expanded rapidly at $\sim$100 km s^{-1} at the start of the flare. After $\sim$20 s, the smaller loop then reconnected with magnetic loops within the arcade, resulting in two new post-reconnection loops. The newly-formed, smaller EUV loop, with a long cusp at the looptop, was also observed in X-rays. The newly-formed, larger loop, visible in EUV and Hα, with a twisted structure and a jagged looptop, expanded outwards at $\sim$490 km s^{-1}. The 6-12 keV image during the first of two hard X-ray peaks showed the two footpoints of the newly-formed, smaller loop and a separate coronal source which was located much higher than the looptop seen later in the same energy band. We speculate that the coronal X-ray source was at or near the initial reconnecting point of the two interacting loops. All these observations indicate: (1) the loop-loop interaction was the trigger of the flare; (2) new loop systems do result from the magnetic reconnection of interacting loops; and (3) the cusp-shaped loops often seen in soft X-rays and EUV can be the product of the interaction of two loops.

Subject headings: Sun: flares—Sun: X-rays

[1]Department of Physics, Catholic University of America, Washington, DC 20064.

[2]Laboratory for Solar and Space Physics, Code 612.1, NASA Goddard Space Flight Center, Greenbelt, MD 20771.

1. Introduction

The interaction of multiple coronal loops has long been considered as a possible mechanism to trigger solar flares. There have been several flare models proposed in this regard (see review by Aschwanden 2004): the merging of two magnetic dipoles with a current sheet formed in between (Sweet 1958), emergence of a small loop reconnecting with an overlying, pre-existing coronal loop (Heyvaerts, Priest, & Rust 1977), converging double-arcade model (Uchida et al. 1999), and the break-out model (Antiochos et al. 1999). Interacting flare loops have been reported in a number of observations (e.g., Kundu 1984; Machado et al. 1988; Sakai & de Jager 1991; Shibata et al. 1992; Strong et al. 1992; Shimojo et al. 1996). With observations in soft and hard X-rays, radio and Hα, Hanaoka (1996, 1997) and Nishio et al. (1997) have found that a typical configuration for flares involving interacting loops consists of two loops of different sizes, which seemed to favor the emerging flux model proposed by Heyvaerts, Priest, & Rust (1977). To explain the 'three-legged structure' in X-ray and radio images, both Hanaoka and Nishio et al. argued that the two post-reconnected loops share one magnetic polarity patch. Nishio et al. (1997) found that microwave emission was seen from both post-reconnected loops, while hard X-ray (HXR) emission is preferentially radiated from the shorter of the two loops. Because a cusp-like structure, which has been seen in some events with Yohkoh (Tsuneta et al. 1992; Tsuneta 1996), was not seen in the flares they analyzed, Hanaoka (1996) and Nishio et al. (1997) argued that there might be two different 'basic flare types': the cusp-shaped single-loop flare and the double-loop flare associated with emerging flux.

The quadrupolar field configuration so far has been reconstructed based solely on post-reconnection observations. As pointed out by Aschwanden (2004, p. 456), the magnetic field configuration before and during reconnection is generally invisible, because it takes tens of seconds to minutes for evaporated chromospheric plasma to fill the loops. Thus, the field lines are not yet 'illuminated' by heated flare plasma. Consequently, the observations previously reported (e.g., Hanaoka 1996, 1997; Nishio et al. 1997) only show post-reconnection configurations in which the newly reconnected, cusp-shaped field lines may have already relaxed into a more rounded, dipolar shape.

In this paper, we report multiwavelength observations of a flare that clearly show loop connectivity changes as a result of a loop-loop interaction. In EUV observations obtained with the Transition Region and Corona Explore (TRACE) in the 195 Å channel, a coronal loop was first seen to expand, and then reconnect with another, larger loop to form a cusp structure at the top of one of the newly-formed loops. X-ray observations obtained with the Ramaty High Energy Solar Spectroscopic Imager (RHESSI) provide the timing of the electron acceleration and the locations of precipitating electrons during this loop reconfiguration process. Hα observations obtained from the Meudon Observatory provide complementary information on an outward moving source in this flare. Because the Large Angle and Spectrometric Coronagraph (LASCO) on board the Solar and Heliospheric Observatory (SOHO) did not have observations from 2002 June 1 to 5, we do not know if there was a coronal mass ejection associated with this flare.

2. Observations and Data Analysis

An M1.0 flare occurred on 2002 June 2 in active region AR 9973 near Sun center (-150″, -300″). The RHESSI X-ray light curves in five energy bands are shown in Figure 1. The start time of the impulsive phase of the flare, defined here as the time when the $>$ 25 keV hard X-ray (HXR) flux increased significantly, was 11:44 UT, within 20 s of the start time of the flare at lower energies. Consequently, we call this flare an "early impulsive flare" (Sui, Holman, & Dennis 2005). The hard X-ray light curves had two peaks. Because the thermal emission was still weak, the first peak can be seen at energies as low as 3-6 keV. This indicates the absence of significant plasma pre-heating to temperature on the order of or greater than 10 MK before particle acceleration. Because of the weak thermal emission at low energies, RHESSI X-ray spectra of this flare have been used to determine the low-energy cutoff to the nonthermal electron distribution (Sui, Holman, & Dennis 2005).

TRACE images in Figure 2 show the evolution of the magnetic loop morphology during the flare. The loop evolution can also be seen in the TRACE 195 Å movie at http://hesperia.gsfc.nasa.gov/~sui/20020602/trace.mpg. In the pre-flare phase, a ribbon-like structure (source A), indicated by an arrow in the first panel of Figure 2, was visible starting at 11:41:12 UT, $\sim$3 min before the start of the flare as seen by RHESSI. This ribbon continually moved toward the right (i.e., the west on the Sun) at a speed of $\sim$6 km s^{-1}. At 11:43:28 UT, two additional sources (Sources B and C as indicated by two arrows in the second panel), appeared to the east of the ribbon. Source C can be identified later as a loop which became evident at 11:44:02 UT, while source B still remained as compact as when it was first formed. The brightness of all three sources increased at 11:44:02 UT, within 2 seconds of the hard X-ray flux increase seen with RHESSI (see Fig. 1), indicating intensified plasma heating. At 11:44:19 UT, Source C (the loop) was expanding toward the southwest at a speed of $\sim$100 km s^{-1} (without consideration of the projection effect). The intensity of all three sources increased significantly. In the meantime, the RHESSI 12-25 keV flux increased impulsively by an order of magnitude above the pre-flare background.

At 11:44:36 UT, the time of the first HXR peak, the expanding loop appeared to break up, with the bottom of the west half of the loop much brighter than its top part. The other half of the loop was invisible in the image. Meanwhile, the brightness of source B increased significantly. The broken-up loop and source B appeared to be unconnected at this time. Since a unipolar loop cannot exist, the broken loop may have been connected to source B at this time, suggesting the loop connectivity change which can be clearly seen at later times. The likely reason the newly reconnected loop was not visible was that it has not yet been filled with sufficient hot, evaporated plasma at the right temperature, i.e., ∼20 MK or 1.5 MK (Handy et al. 1999), to produce 195 Å emission. The brightness of the ribbon (source A) also increased, but it was not as bright as the broken-up loop and source B at this time. An additional source (source D) appeared to the south of all the sources introduced above. Since the flare was located in the southern hemisphere, taking into account the projection effect, source D was most probably located higher than sources A, B and C. It later evolved to be a large, twisted loop-like structure moving outward. At 11:44:53 UT, the second HXR peak, the upper part of the broken-up loop was moving toward the west, i.e., toward source B, with its bottom still much brighter than its top part, consistent with intense heating by nonthermal particles. Source B maintained its high brightness, while the brightness of the ribbon (source A) seemed to decrease. Because of the existence of the TRACE diffraction pattern in the image, the newly-formed, smaller loop was not fully visible until 11:45:10 UT. Meanwhile, a cusp-shaped structure appeared above the newly-formed loop. The bottom part of the newly-formed loop was still brighter than the upper part and the cusp. At 11:45:27 UT, the outermost layer of the loop appeared to be sharp and bright, and it extended up to the tip of the cusp, suggesting the recently-reconnected, hottest loop as a result of the most intensive heating at the time of the HXR peak. After 11:45:27 UT, the brightness of the top part of the newly-formed loop increased gradually. This is presumably due to the continuous buildup of heated chromospheric plasma in the loop. Meanwhile, the brightness of the ribbon (source A) continued to decrease.

The larger but fainter loop (source D) that formed well above the newly-formed, smaller loop had a rather complicated shape, because (a) it appeared twisted and (b) it had a very jagged looptop. It moved upward at ∼490 km s^{-1}. In the images from 11:45:10 through 11:45:44 UT, this loop appeared to have its own cusp-like structure that eventually pointed radially outward. This structure was most likely an artifact resulting from the small observation angle to the plane containing the loop and from the twist of the loop, which resulted in the loop not being contained within a single plane. The images also indicate that some pre-existing overlying loops (which may not have been involved in the magnetic reconnection) expanded outwards with the newly-reconnected loop. The linear, not quite horizontal structure located near x=-170″, y=-335″ in the images at 11:44:53 and 11:45:10 UT indicates the presence of these overlying loops. Because there is a ∼4 min data gap after 11:45:44 UT, no further information on this upward moving loop can be obtained from TRACE. The cusp structure above the newly-reconnected, smaller loop could still be seen at 11:49:19 UT, even after the X-ray flux below 25 keV had decreased to near preflare background levels. At that time, the ribbon (source A) was invisible. After another ∼4 min data gap, the cusp had disappeared. The images later show a typical post-flare loop with multiple strands (or an arcade of loops).

Further information on the outward moving, twisted, large-scale loop-like source (source D) can be obtained from the Meudon Hα observations (in the blue wing at 6563.3 Å). Two sample images are shown in Figure 3. The bright, loop-like source in Hα corresponds to the newly-formed, smaller loop seen in the TRACE images. The dark, outward moving loop-like source in Hα absorption is likely to correspond to the newly-formed, larger loop (source D) in the TRACE images, because they appeared almost at the same time and at the same location. When moving outwards, the large, dark loop in Hα appeared larger, with the top of the loop much thicker than the two legs. The west leg of the loop seems to be anchored near the EUV ribbon (source A), while the east leg seems to be anchored near the east footpoint of the emerging, pre-existing loop (source C). After moving for ∼10 minutes the large loop became very dim and eventually disappeared from the image.

The RHESSI images in all energy bands up to 50-100 keV first show two separated sources. As shown in panel A of Figure 4, the RHESSI images in three energy bands, i.e., 6-12, 12-25 and 25-50 keV, all show two sources at the first HXR (>25 keV) peak. They are co-spatial with the two bright sources seen in the TRACE image at 11:44:36 UT, indicating that they are the footpoints of the newly reconnected, smaller loop. The two bright footpoints seen with TRACE were presumably the result of intense heating by the energetic electrons. Emission at 6-12 keV usually originates from hot flare loops, so it is unusual that the 6-12 keV images in this flare show two footpoints. However, this observation is consistent with the very short plasma pre-heating phase in this flare. The accelerated low-energy electrons can travel down to the footpoints through the relatively cool, low-density loop. Moreover, the 6-12 keV image shows an additional source apparently located in the corona. This coronal source appears to be close to, but northwest of the top of the broken-up loop (source C) seen in TRACE. No X-ray emission was seen along the TRACE ribbon (whose brightness started to decrease after 11:44:36 UT, see Fig. 2) and the east leg of the broken-up loop (which was also invisible in the TRACE images).

The 12-25 and 25-50 keV images at the second HXR peak (11:44:48 UT), as shown in panel B in Fig. 4, still show two footpoints, and they are still co-spatial with the two bright TRACE footpoints. Different from the earlier time, the 6-12 keV image shows a loop-like structure instead, suggesting that evaporated plasma heated by energetic electrons at the footpoints had filled the newly-formed loop. The separate coronal source seen earlier was not visible at this time. After the second HXR peak, the >25 keV HXR flux decreased quickly. The images below 25 keV, such as those shown in panel C of Figure 4, now show a coronal source located at the top of the newly-formed, smaller loop. During that time, the brightness of the two loop footpoints seen in the TRACE images decreased significantly. This is presumably because of the absence of the nonthermal particles. The transition of the soft X-rays (i.e., 6-12 keV) origin from impulsive footpoints to a coronal source in this event was reported by Veronig et al. (2005), when they used this event to study the Neupert effect. They argued that this observation supports chromospheric heating by nonthermal particles. Recently Liu et al. (2005) reported RHESSI observations showing that the soft X-ray sources gradually moved from the bottom to the top of a loop in another flare.

3. Summary and Discussions

We consider that the observations presented here strongly support the two-loop interaction as the trigger of the flare. In order to better show the loop connectivity change during the flare, three images with a smaller field of view are shown in the upper row of Fig. 5. These three images are at early rise phase (left panel), start of impulsive phase (right panel), and decay phase (right panel) of the flare. Our suggested loop configurations corresponding to these three time periods are shown in the bottom row of Fig. 5. They illustrate the loop connectivities before, at the start of and after magnetic reconnection. When the flare started, one smaller loop (source C) expanded (or emerged) quickly toward the southwest at $\sim$100 km s^{-1} (bottom left panel of Figure 5). This rapidly expanding loop collided with a loop arcade (bottom middle panel), leading to magnetic reconnection which resulted in particle acceleration and intensive plasma heating. The magnetic reconnection formed one small loop system connecting the two neighboring polarities, and a larger loop connecting the two distant polarities (bottom right panel). Accelerated electrons preferentially propagated along the smaller loop to the chromosphere, resulting in intense heating and chromospheric evaporation at the footpoints of that loop. In the meantime, the newly-formed larger loop expanded upward.

The magnetogram obtained with the Michelson Doppler Imager (MDI) on board SOHO supports this quadrupolar interpretation. As shown in Figure 6, the region 1 (R1, where source A was located) is an elongated area with negative polarity, whose shape is very similar to source A (EUV ribbon). Region 2 (R2, where source B was located) is a compact region with positive polarity. Region 3 (R3) and region 4 (R4) have opposite polarities and were connected with the smaller loop (source C) before the flare. After reconnection, R2 and R3 were connected through the newly-formed smaller loop, while R1 and R4 were connected with the newly-formed larger loop (source D). Notice that region R2 and R3 are co-spatial with the two HXR footpoints in Fig. 6.

The observations of this flare have two important implications. First, flares having only one soft X-ray loop and two HXR footpoints may not be 'simple two-footpoint' flares as Krucker & Lin (2002) reported for this flare. Instead, they may be the result of a loop-loop interaction, as shown here. The flare loop and footpoints seen in X-rays could just be the newly-formed smaller loop, which contains the highest flux of nonthermal electrons. The other newly-formed larger loop is invisible in X-rays because very few accelerated electrons were injected into that loop, resulting in insufficient plasma temperatures and emission measures. This agrees with the findings of Nishio et al. (1997) that HXRs are preferentially emitted from shorter loops. Secondly, flares showing a cusp structure could be triggered by a two-loop interaction. Aschwanden et al. (1999) have pointed out that the three-dimensional quadrupolar geometry implies the formation of cusp-shaped field lines. So cusp-shaped single-loop flares may often be a special case of quadrupolar reconnection, when only the post-reconnected small loop is visible in soft X-rays and the large-scale loop is undetected. This is consistent with our observations. Therefore, the two different 'basic flare types' suggested by Hanaoka (1996) and Nishio et al. (1997), i.e., double-loop flares with emerging flux and cusp-shaped single-loop flares, may be in fact the same. The resason no cusp-shaped structure was seen in the events analyzed by Hanaoka (1996, 1997) and Nishio et al. (1997) could be due to the length of the shorter loop observed in soft X-rays being smaller than the resolution capability of Yohkoh/SXT. No high-resolution EUV data was available for their analysis.

Several aspects of the observations are worth discussing here:

1. Plasma heating could occur before the reconnection starts. The loop connectivity change occurred at ∼11:44:19 UT, suggesting that magnetic reconnection occurred at this time. The appearance of sources A, B, and C in EUV and their gradual brightness increase as early as ∼3 min before the reconnection indicate slow plasma heating before magnetic reconnection. This slow heating process did not produce hot enough plasma to be seen in soft X-rays.

2. Particle acceleration could occur before the cusp formation. The EUV cusp was not clearly visible until 11:45:10 UT, which is ∼30 s after the HXR flux increase. Before that time (from 11:44:36 to 11:45:10 UT), the upper part of the apparently broken-up loop was moving toward the west until the cusp was formed. This could suggest that the particle acceleration occurred even before the formation of the cusp. It is also possible that the cusp formed before 11:44:36 UT, but was too hot to be seen in EUV and/or the emission measure was too small.

3. The initial site of magnetic reconnection between the two colliding loops may have been seen by RHESSI. At the time of the first HXR peak, the RHESSI 6-12 keV images show two footpoints and an additional coronal source. The separate coronal source was located much higher ($\sim$14 arcsec) than the loop-top source seen in the RHESSI image at 11:45:20 UT. It appeared to be located near the tip of the cusp. Furthermore, it was seen in the time interval when reconnection presumably just started. Consequently, we speculate that the source represents the colliding point of the two interacting loops. It is also possible that this coronal source is equivalent to the HXR Masuda sources (Masuda et al. 1994), except the Masuda source was in >20 keV HXRs. The reason we could not see the coronal source at the second HXR peak could be due to the limited dynamic range of RHESSI images. Such a source was not seen in the flares reported by Hanaoka (1996, 1997) and Nishio et al. (1997). Its appearance here could be due to RHESSI's broader energy coverage than that of the Yohkoh Hard X-ray Telescope (HXT). Yohkoh/HXT did not cover the energy range between 3 and 14 keV.

4. The emerging loop does not have to be under the large loop to trigger the flare. In this case, the small loop emerged beside the large loop arcade and expanded toward it at the start of the flare. Moreover, the two post-reconnection loops did not share a single magnetic polarity patch. These are different from the pre- and post-reconnection loop configurations suggested by Hanaoka (1997) and Nishio et al. (1997) for the flares they analyzed.

Finally, we point out that the observations of this flare do not fit any of those currently popular models for eruptive events, such as the flux rope model (e.g., Cargill & Priest 1983; Lin & Forbes 2000), which only involves a dipolar field, and the break-out model (Antiochos et al. 1999), which requires the shearing and eruption of an arcade of loops in the middle. Instead, we found that the 'old' two-loop interaction model (e.g., Heyvaerts, Priest, & Rust 1977) fits the observations better. Certainly, the traditional 2D loop interaction model needs to be expanded to 3D in order to explain some of observations presented here, such as the outward-moving, twisted coronal loop with a jagged looptop.

We acknowledge helpful discussions with Jiong Qiu and Markus J. Aschwanden. We thank Jean-Marie Malherbe for providing the Meudon Hα data. We also thank the TRACE and RHESSI teams for their hard work and the open data policies that made this study possible. Both TRACE and RHESSI are NASA Smaller Explorer Missions. This work was supported in part by NASA SEC Guest Investigator Grant 370-16-20-16 and by the RHESSI project.

REFERENCES

Antiochos, S. K., DeVore, C. R., Klimchuk, J. A. 1999, ApJ, 510, 485

Aschwanden, M. J. 2004, Physics of the Solar Corona, Springer Pub.

Aschwanden, M. J., Kosugi, T., Hanaoka, Y., Nishio, M. & Melrose, D. B. 1999, ApJ, 526, 1026

Cargill, P. J., & Priest, E. R. 1983, ApJ, 266, 383

Hanaoka Y. 1996, Sol. Phys., 165, 275

Hanaoka Y. 1997, Sol. Phys., 173, 319

Handy, B.N., Acton, L.W., Kankelborg, C.C. et al. 1999, Sol. Phys., 187, 229

Heyvaerts, J., Priest, E. R., and Rust, D. M. 1977, ApJ 216, 123

Krucker, S., & Lin, R. P. 2002, Sol. Phys., 210, 229

Kundu, M. 1984, Adv. Space. Res., 4(7), 157

Lin, J., & Forbes, T.G. 2000, J. Geophys. Res., 105, 2375

Liu, W., Liu, S., Jiang, Y., Petrosian, V., 2005, American Geophysics Meeting, SP41C06

Machado, M. E., Moore, R. L., Hernandez, A. M., Rovira, M. G., Hagyard, M. J., and Smith, Jr. J. B. 1988, ApJ, 326, 425

Masuda, S., Kosugi, T., Hara, H., Tsuneta, S., & Ogawara, Y. 1994, Nature, 371, 495

Nishio, M., Yaji, K., Kosugi, T., Nakajima, H., & Sakurai, T. 1997, ApJ, 489, 976

Sakai, J. & de Jager, C. 1991, Sol. Phys., 134, 329

Shibata, K., et al. 1992, ApJ, 44, L173

Shimojo, M., Hashimoto, S., Shibata, K., Hirayama, Y., Hudson, H. S., & Acton, L. W. 1996, PASJ, 48, 123

Strong, K. T., Harvey, K. L., Hirayama, T., Nitta, N., Shimizu, T. & Tsuneta, S. 1992, PASJ, 44, L161

Sui, L., Holman, G. D., & Dennis, B. R. 2005, American Geophysics Meeting, SP41C03

Sweet, P. A. 1958, The production of high-energy particles in solar flares, Nuovo Cimento Suppl. 8, Ser. X, 188-196

Tsuneta, S. 1996, ApJ, 456, 840

Tsuneta, S., Hara, H., Shimizu, T., Acton, L.W., Strong, K.T., Hudson, H.S., & Ogawara, Y. 1992, PASJ, 44, 63

Uchida, Y., Hirose, S., Cable, S., Morita, S., Torii, M., Uemura, S., Yamaguchi, T. 1999, Publ. of the Astronomical Society of Japan, 51, 553

Veronig, A. M., Brown, J. C., Dennis, B. R., Schwartz, R. A., Sui, L., Tolbert, A. K. 2005, ApJ, 621, 482

This preprint was prepared with the AAS LaTeX macros v5.2.

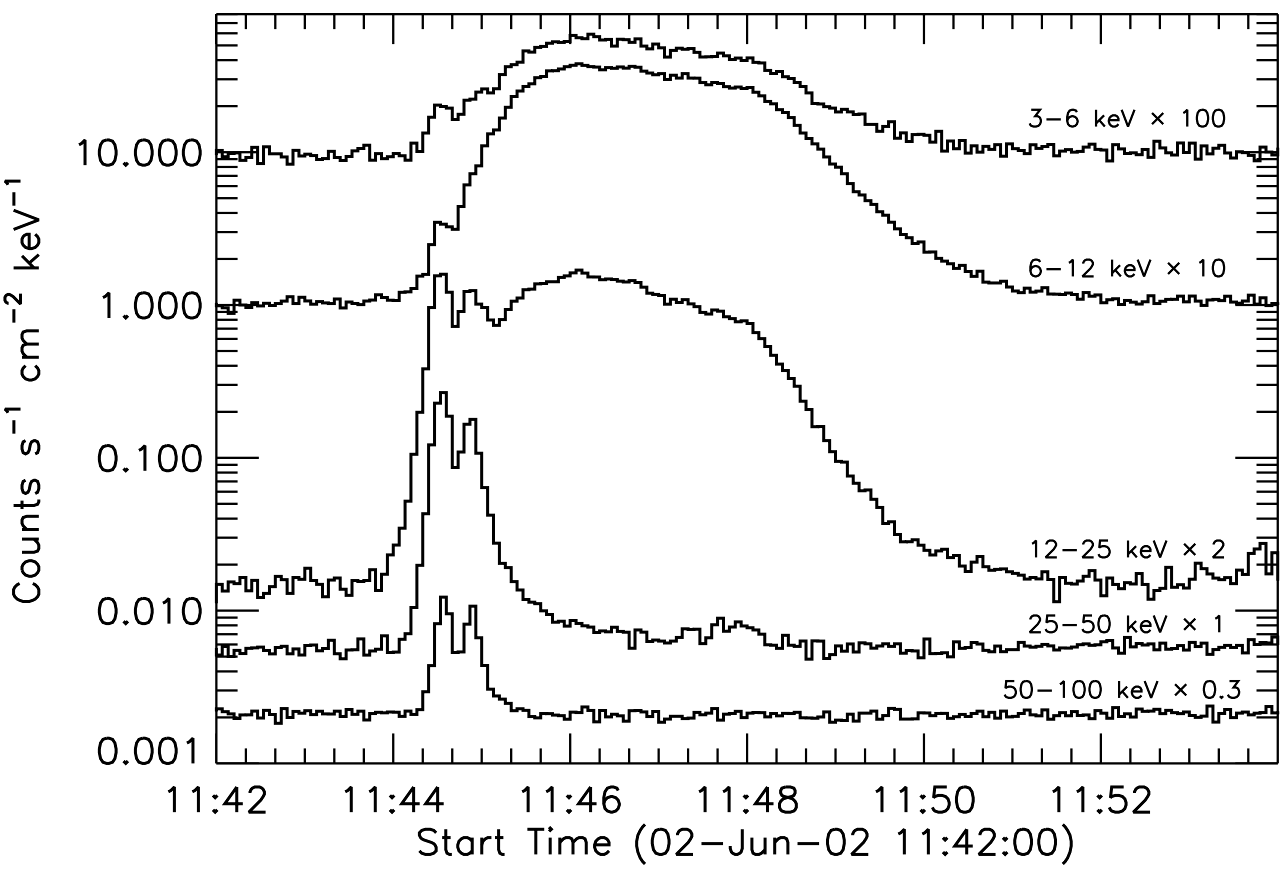

Fig. 1.— RHESSI light curves in five energy bands. The time resolution is 4 s.

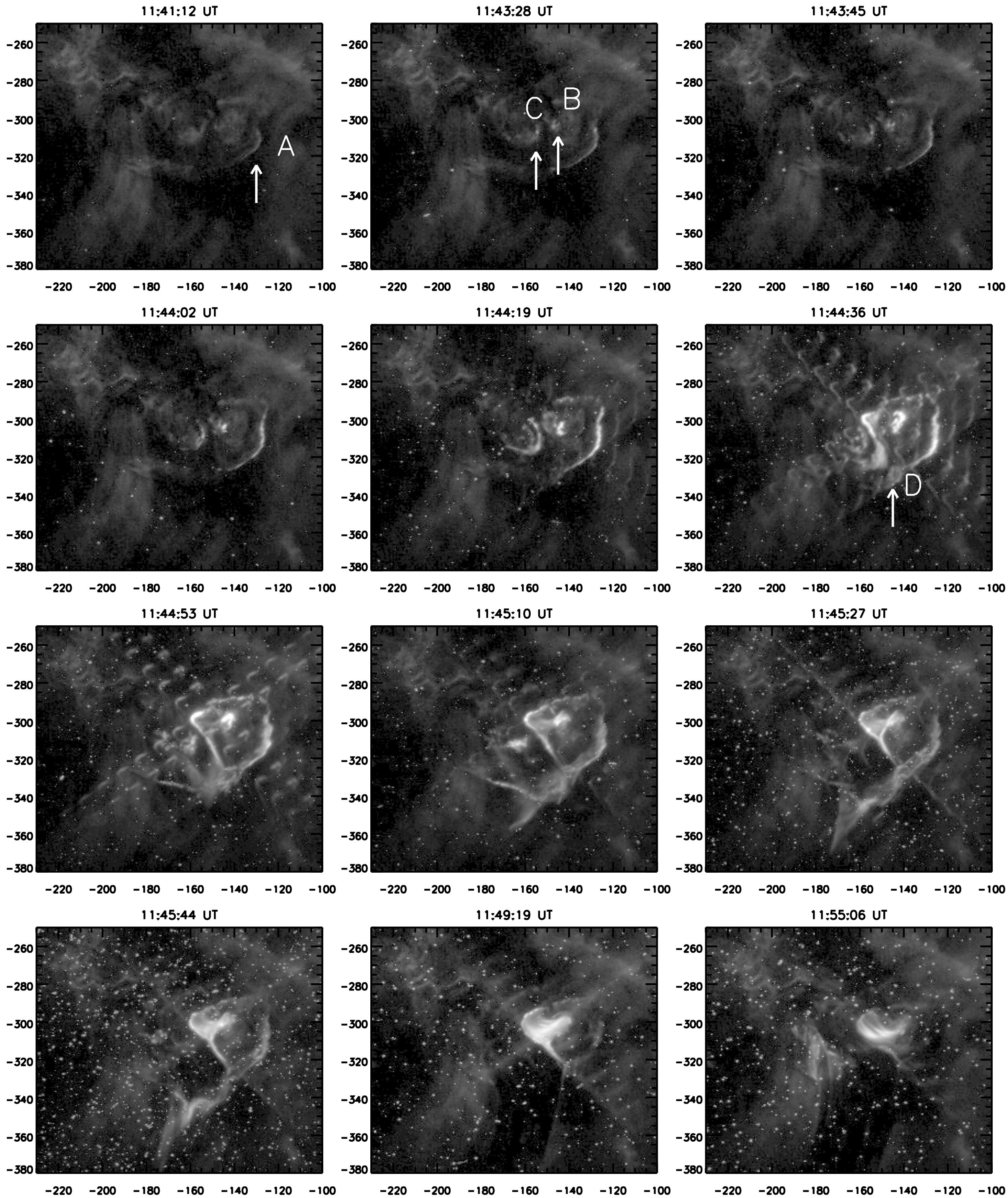

Fig. 2.— TRACE 195 Å images of the 2002 June 2 flare. The images were shifted (x:+5″, y:-5″) to co-align with RHESSI images. The exposure time of each image is ∼10 s. The noise spikes in the images are not filtered out, because we found removing the spikes changes some details in the images.

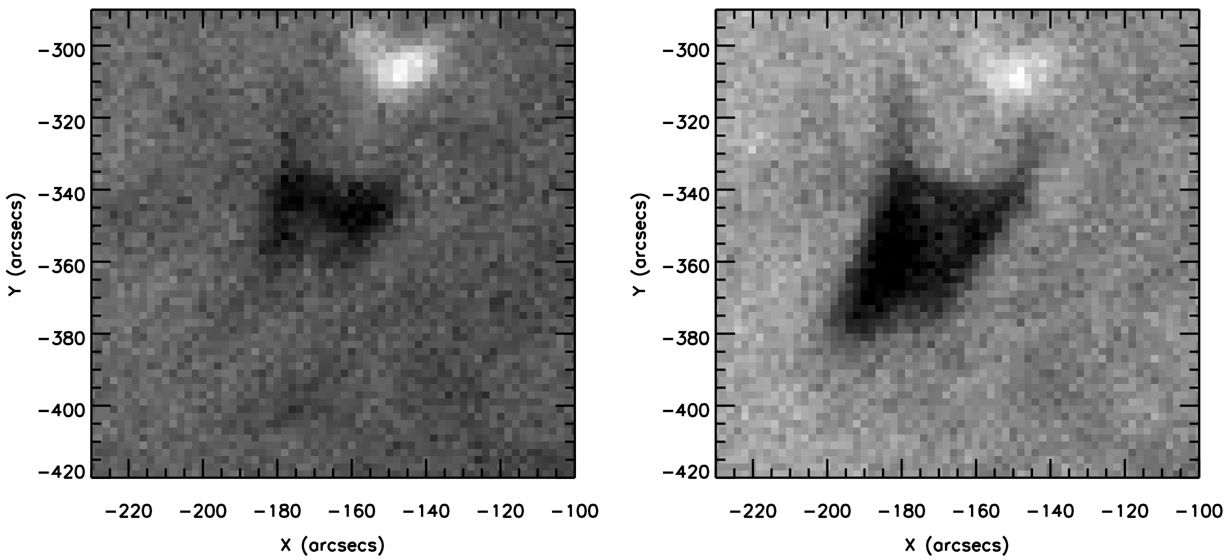

Fig. 3.— Two sample Hα blue wing (6563.3 Å) images at 11:48:52 UT (left panel) and 11:51:59 UT (right panel) obtained from Meudon Observatory. Because of pointing uncertainties, the images were shifted to co-align the loop seen in Hα emission with the newly-formed compact loop seen in RHESSI and TRACE images.

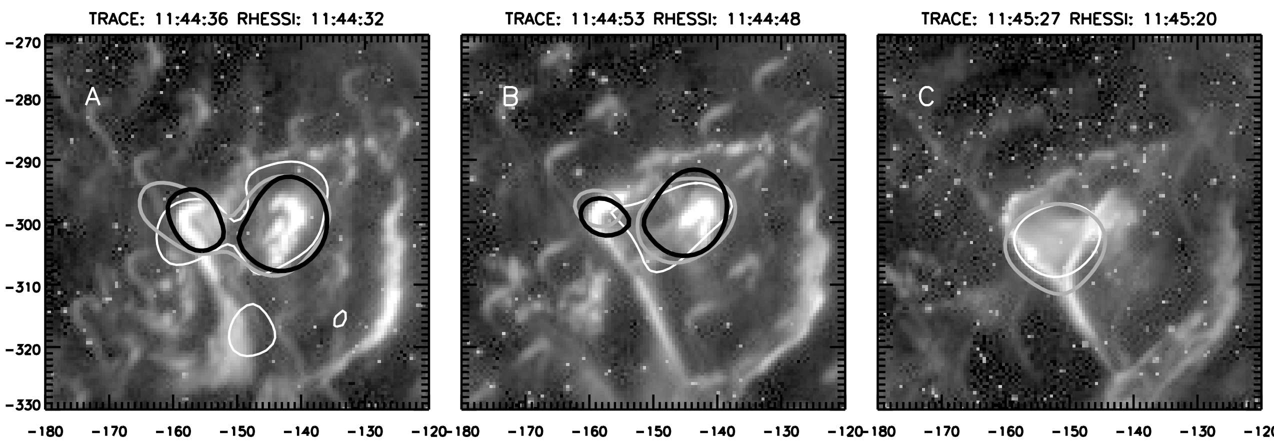

Fig. 4.— RHESSI images overlaid on top of TRACE images. In three panels, the white (50% of the peak flux), gray (40%) and black (40%) contours are RHESSI 6–12, 12–25, and 25–50 keV images, respectively. No 25-50 keV image is shown in panel C because of the absence of HXR flux by that time. The RHESSI images were constructed with the CLEAN algorithm using detectors 3-9, giving a spatial resolution ∼7 arcsec. The integration time of each RHESSI image is 8 s. The TRACE images were shifted (x:+5″, y:-5″) to co-align with RHESSI images.

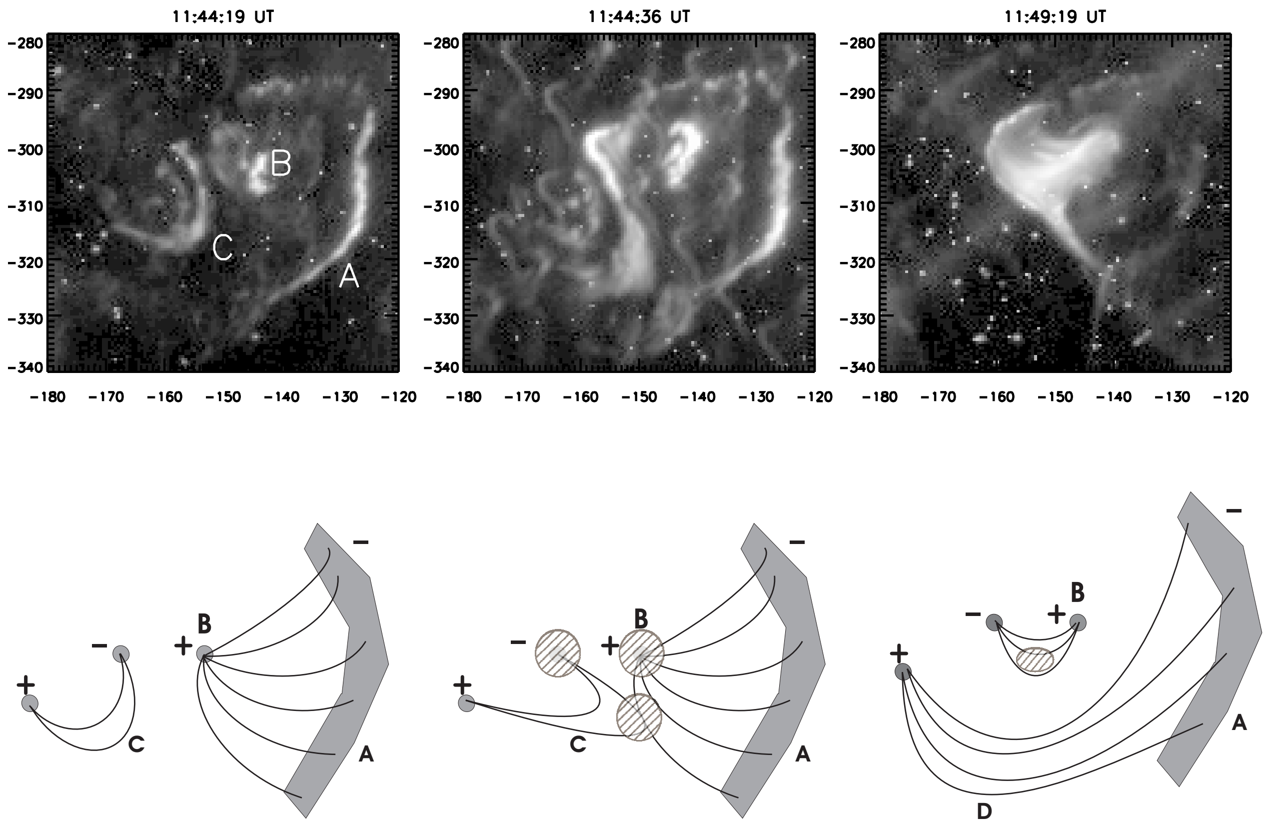

Fig. 5.— Upper row: TRACE 195 Å images with the smaller field of view at early rise phase (left Panel), start of impulsive phase (middle panel), and decay phase (right panel) of the flare. Bottom row: schematic illustrations of loop configurations corresponding to the three time periods. They show the loop connectivities before (left panel), at the start of (middle panel) and after (right panel) magnetic reconnection. Sources A, B, and C correspond to the EUV sources in the upper row. Source D can be seen in the TRACE images in Fig. 2. The circles filled with black stripes in the cartoon indicate regions emitting 6-12 keV X-rays. The information of magnetic polarity is based on the SOHO/MDI magnetogram shown in Fig. 6.

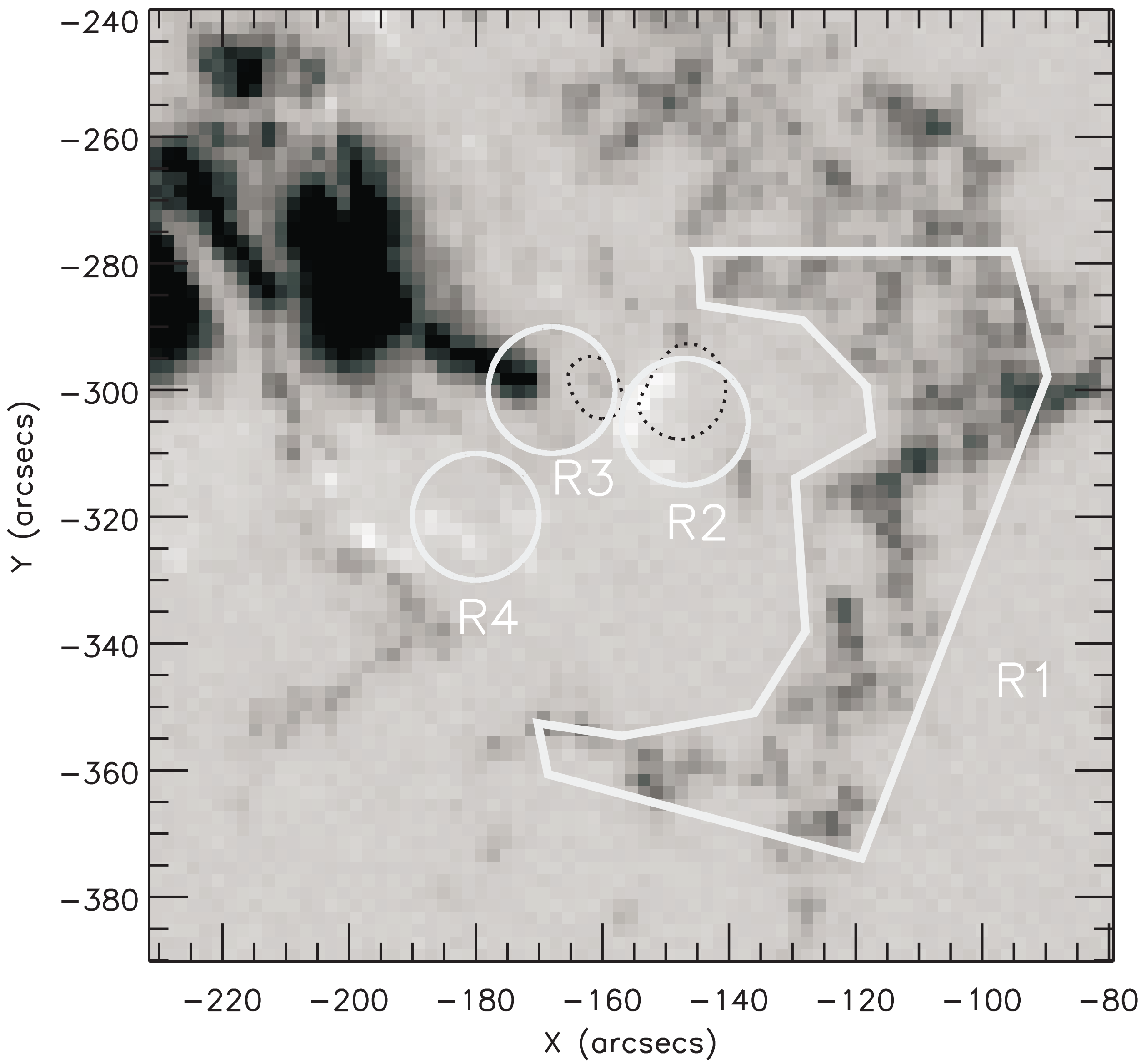

Fig. 6.— Magnetogram obtained with SOHO/MDI at 11:21 UT. Four regions (from R1 to R4) were involved in the flare. The dotted contours show 40% of the peak flux in the RHESSI 25-50 keV image at 11:44:32 UT.